

Comparing the use of two kinds of droop control under microgrid islanded operation mode

DENGKE GAO, JIANGUO JIANG, SHUTONG QIAO

*Key Laboratory of Control of Power Transmission and Conversion
Shanghai Jiao Tong University, Ministry of Education
800 DongChuan Road, MinHang District, Shanghai, P.R. China, 200240
e-mail: gaodengke@gmail.com*

(Received: 11.05.2012, revised: 28.01.2013)

Abstract: A microgrid with parallel structure operating under islanded mode is considered in this paper. Under microgrid islanded operation mode, lines bring adverse effect for power distribution between microsources (MSs). Because traditional droop control ignores this effect, MSs adopting this method can not achieve satisfactory power distribution. A kind of droop control including line compensation applied to this microgrid is proposed. It can eliminate this effect to obtain satisfactory power distribution. The relationship of two kinds of droop control with power distribution is analyzed. The reference voltage generated by droop control is applied to control output voltage of MSs. Comparison of two kinds of droop control through MATLAB/Simulink simulation is made to verify the superiority of droop control including line compensation for power distribution. The relationship between PCC voltage and output power of MSs is also presented.

Key words: microgrid, microsource, droop control, power distribution

1. Introduction

Microgrid is composed by microsources (MSs), loads, power electronic converters and so on to constitute a controllable system. It can not only utilize the advantage of distributed generation (DG) but also overcome the disadvantage of DG for distribution network. So it is beneficial for extensive application of renewable energy generation. Its energy is mainly provided by photovoltaic cell, wind turbine, fuel cell and microturbine. Moreover, its energy is mainly stored by battery, supercapacitor and flywheel. It may run under grid-connected operation mode or islanded operation mode [1-6]. In this paper, only microgrid islanded operation mode is considered.

Under microgrid islanded operation mode, the voltage support of microgrid is supplied by MSs. It is required to share load power between MSs to achieve power balance. The power distribution between MSs is usually according to the ratio of their nominal apparent power. Because droop control dose not need communication between MSs to realize this function,

it was widely used in designing MS controller in [7-10]. Lines bring adverse effect for power distribution between MSs [11, 12]. However, this kind of droop control does not consider this adverse effect and is called as traditional droop control in this paper. As an improvement of traditional droop control, droop control considering line adverse effect was introduced in [13, 14]. It can eliminate the adverse effect from lines to let MSs obtain satisfactory power distribution and is called as droop control including line compensation in this paper.

This paper proposes a kind of droop control including line compensation used for microgrid with parallel structure. The relationship of two kinds of droop control with power distribution between MSs is theoretically analyzed. The design procedure of MS controller with droop control is also presented. Comparing the use of two kinds of droop control is done through simulation with MATLAB/Simulink.

2. Microgrid structure

The microgrid structure considered by this paper is shown in Figure 1. It mainly consists of three distributed MSs with their own lines, i.e. MS1-3 with line1-3, and one centralized load. Three MSs are parallel with the load at the point of common coupling (PCC) through line1-3. Microgrid can run under grid-connected operation mode through a closed static transfer switch (STS). When this switch is open, microgrid will run under islanded operation mode without any connection with the grid. This paper only pays attention to the use of droop control under microgrid islanded operation mode in a three phase symmetrical system with voltage level of 380 V.

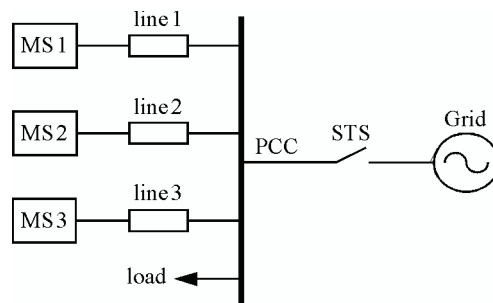


Fig. 1. Microgrid structure

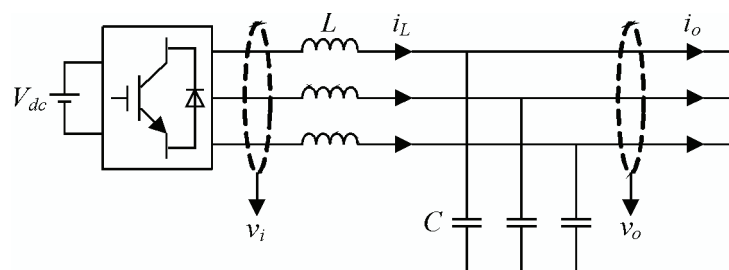


Fig. 2. MS structure

MS structure is shown in Figure 2. It is constituted by DC bus side, inverter and *LC* filter. The voltage of its DC bus side is jointly decided by distributed energy sources and energy storage equipments through power electronic converters. Since this voltage can be controlled by converters to be basically stable, the DC bus side of MS is represented by a DC voltage source with voltage V_{dc} in this paper so as to simplify analysis. So the control of MS is simplified to control the inverter. In Figure 2, v_i and v_o are inverter output voltage and MS output voltage, i_L and i_o are inductance current and MS output current.

3. Droop control and power distribution

This part presents two kinds of droop control, i.e. traditional droop control and droop control including line compensation. Traditional droop control does not take into account line adverse effect, but droop control including line compensation attempts to eliminate this effect. The requirements for achieving expected power distribution between MS1-3 are demonstrated. Through this expression, it is theoretically revealed that droop control including line compensation can bring better power distribution.

A) Traditional droop control and power distribution

Through analysis of Figure 1, the out power of MS in a three phase symmetrical system can be expressed as

$$\begin{cases} P_o = \frac{V_o E \cos(\delta - \delta_e - \varphi) - E^2 \cos \varphi}{|Z|/3} \\ Q_o = \frac{-V_o E \sin(\delta - \delta_e - \varphi) - E^2 \sin \varphi}{|Z|/3}, \end{cases} \quad (1)$$

where P_o and Q_o are MS output real power and reactive power, V_o and E are RMS of MS output voltage and PCC voltage, δ and δ_e are phase angle of MS output voltage and PCC voltage, $|Z|$ and φ are line impedance value and angle, line impedance $Z = R + j X$, R and X are line resistance and reactance.

In a low voltage microgrid, Z is nearly resistive [15-17]. As a result, $|Z|$ and φ can be approximated as R and 0. In addition, the voltage phase angle difference $\delta - \delta_e$ is usually very small so as to $\sin(\delta - \delta_e)$ and $\cos(\delta - \delta_e)$ can be replaced by $\delta - \delta_e$ and 1, hence following relationship can be gained from Equation (1)

$$\begin{cases} V_o = E + \frac{RP_o}{3E} \\ \delta = \delta_e - \frac{RQ_o}{3V_o E}. \end{cases} \quad (2)$$

Since V_o and E are almost constant, it can be seen from Equation (2) that V_o is mainly influenced by P_o and δ is mainly influenced by Q_o . Consequently, traditional droop control can be derived by introducing negative feedback with V_o and δ as following equation

$$\begin{cases} V_o^* = V_{oref} - mP_o \\ \delta^* = \delta_{ref} + nQ_o, \end{cases} \quad (3)$$

where V_o^* and δ^* are MS output voltage RMS reference and phase angle reference, V_{oref} and δ_{ref} are MS output voltage RMS reference and phase angle reference when there is no load, m and n are droop coefficients of voltage RMS and phase angle.

To attain power distribution between MS1-3 according to the ratio of their nominal apparent power S , droop coefficients should satisfy following relationship as [18]

$$\begin{cases} m_1S_1 = m_2S_2 = m_3S_3 \\ n_1S_1 = n_2S_2 = n_3S_3. \end{cases} \quad (4)$$

Real power distribution between MS1-3 is analyzed. Following voltage RMS relationship can be derived from Equation (2)

$$\begin{cases} V_{o1} - V_{o3} = \frac{R_1 P_{o1}}{3E} - \frac{R_3 P_{o3}}{3E} \\ V_{o2} - V_{o3} = \frac{R_2 P_{o2}}{3E} - \frac{R_3 P_{o3}}{3E}. \end{cases} \quad (5)$$

In Equation (3), V_o will be seen to as V_o^* if voltage control is desirable. Hence, following voltage RMS relationship can also be obtained

$$\begin{cases} V_{o1} - V_{o3} = -m_1 P_{o1} + m_3 P_{o3} \\ V_{o2} - V_{o3} = -m_2 P_{o2} + m_3 P_{o3}. \end{cases} \quad (6)$$

The left hand side of Equations (5) and (6) is identical, so the output real power of MS1-3 has following relationship

$$\begin{cases} \left(\frac{R_1}{3E} + m_1 \right) P_{o1} = \left(\frac{R_3}{3E} + m_3 \right) P_{o3} \\ \left(\frac{R_2}{3E} + m_2 \right) P_{o2} = \left(\frac{R_3}{3E} + m_3 \right) P_{o3}. \end{cases} \quad (7)$$

Therefore, real power distribution between MS1-3 is

$$\begin{cases} P_{o1} / P_{o3} = \left(\frac{R_3}{3E} + m_3 \right) / \left(\frac{R_1}{3E} + m_1 \right) \\ P_{o2} / P_{o3} = \left(\frac{R_3}{3E} + m_3 \right) / \left(\frac{R_2}{3E} + m_2 \right). \end{cases} \quad (8)$$

In this equation, if real power distribution between MS1-3 is required to according to the ratio of their nominal apparent power, i.e. P_{o1}/P_{o3} and P_{o2}/P_{o3} are equal to S_1/S_3 and S_2/S_3 , following relationship can be gotten through calculation with Equations (4) and (8)

$$R_1S_1 = R_2S_2 = R_3S_3. \quad (9)$$

This relationship indicates that Equations (4) and (9) are both needed to achieve real power distribution between MS1-3 as the ratio of their nominal apparent power. It is easy to fulfill Equation (4) through selection of droop coefficients. However, Equation (9) is usually not satisfied in practice with random line length. Therefore, traditional droop control is difficult to acquire expected real power distribution due to the limitation of Equation (9). Reactive power distribution has similar analysis and conclusion.

B) Droop control including line compensation and power distribution

Because power flows through line, voltage RMS difference $V_o - E$ and voltage phase angle difference $\delta - \delta_e$ satisfy following relationship

$$\begin{cases} V_o - E = \frac{RP_o + XQ_o}{3E} \\ \delta - \delta_e = \frac{XP_o - RQ_o}{3V_o E}. \end{cases} \quad (10)$$

In Equation (10), V_o and E can be approximately taken as 220 V. Then droop control including line compensation can be gained by compensating $V_o - E$ and $\delta - \delta_e$ into Equation (3), that is adding $V_o - E$ and $\delta - \delta_e$ to V_o^* and δ^* in Equation (3) to get new V_o^* and δ^*

$$\begin{cases} V_o^* = V_{oref} - (m - R/660)P_o + XQ_o/660 \\ \delta^* = \delta_{ref} + XP_o/145200 + (n - R/145200)Q_o. \end{cases} \quad (11)$$

From Equation (10), following voltage RMS relationship exists

$$\begin{cases} V_{o1} - V_{o3} = \frac{R_1P_{o1} + X_1Q_{o1}}{660} - \frac{R_3P_{o3} + X_3Q_{o3}}{660} \\ V_{o2} - V_{o3} = \frac{R_2P_{o2} + X_2Q_{o2}}{660} - \frac{R_3P_{o3} + X_3Q_{o3}}{660}. \end{cases} \quad (12)$$

Similar to Equation (6), following voltage RMS relationship derives from Equation (11)

$$\begin{cases} V_{o1} - V_{o3} = -\left(m_1 - \frac{R_1}{660}\right)P_{o1} + \frac{X_1Q_{o1}}{660} + \left(m_3 - \frac{R_3}{660}\right)P_{o3} - \frac{X_3Q_{o3}}{660} \\ V_{o2} - V_{o3} = -\left(m_2 - \frac{R_2}{660}\right)P_{o2} + \frac{X_2Q_{o2}}{660} + \left(m_3 - \frac{R_3}{660}\right)P_{o3} - \frac{X_3Q_{o3}}{660}. \end{cases} \quad (13)$$

Combining Equations (12) and (13), following relationship can be gotten

$$m_1 P_{o1} = m_2 P_{o2} = m_3 P_{o3}. \quad (14)$$

This equation demonstrates that $P_{o1}/P_{o2}/P_{o3}$ equals $S_1/S_2/S_3$ when m is in accordance with Equation (4). It is shown that droop control including line compensation can accomplish expected real power distribution between MS1-3 without dependence on line. Apparently, situation of reactive power distribution between MS1-3 is similar.

4. MS controller design

The content of this part is to design MS controller with droop control. MS controller structure is shown in Figure 3. The control objective of MS is to let its output voltage track its output reference voltage produced by droop control. To realize this aim, following processes with step by step should be adopted.

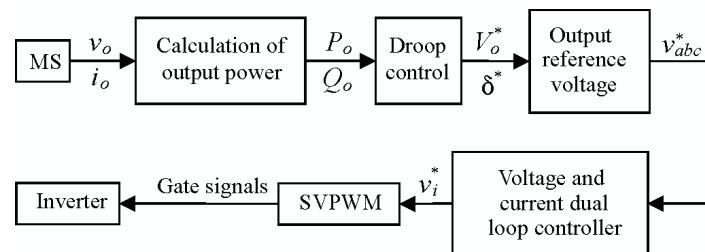


Fig. 3. MS controller structure

Firstly, the measurement value of v_o and i_o from MS output side is used to calculate corresponding P_o and Q_o as Equation (15)

$$\begin{cases} P_o = \frac{\omega_c}{s + \omega_c} (v_{od} i_{od} + v_{oq} i_{oq}) \\ Q_o = \frac{\omega_c}{s + \omega_c} (v_{oq} i_{od} - v_{od} i_{oq}), \end{cases} \quad (15)$$

where v_{od} and v_{oq} are d axis and q axis component of v_o , i_{od} and i_{oq} are d axis and q axis component of i_o , ω_c is cutoff frequency of first order low-pass filter.

Secondly, calculation of V_o^* and δ^* based on droop control with Equations (3) or (11) is used to get the three phase output reference voltage v_{abc}^* of MS with 100π rad/s angular frequency as following equation

$$\begin{cases} v_a^* = \sqrt{2} V_o^* \cos(100\pi t + \delta^*) \\ v_b^* = \sqrt{2} V_o^* \cos(100\pi t + \delta^* - 2\pi/3) \\ v_c^* = \sqrt{2} V_o^* \cos(100\pi t + \delta^* + 2\pi/3). \end{cases} \quad (16)$$

Then, this reference voltage is used to gain the reference voltage v_i^* of inverter through a voltage and current dual loop controller [19]. It incorporates voltage outer loop controller and current inner loop controller and is shown in Figure 4.

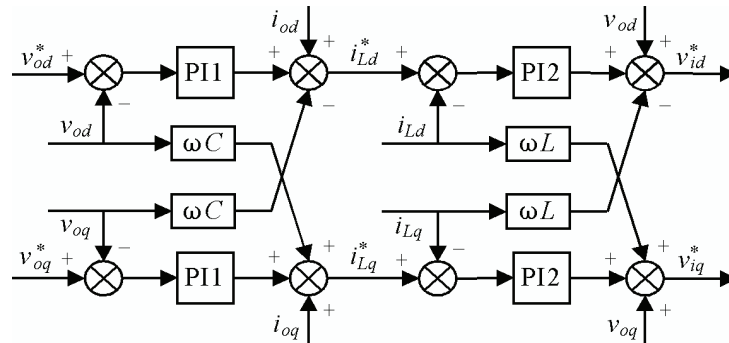


Fig. 4. Voltage and current dual loop controller

Voltage outer loop controller utilizes the error between v_{abc}^* and v_o with feedforward decoupling and PI control to get the inductance reference current i_L^* as Equation (17)

$$\begin{cases} i_{Ld}^* = i_{od} - \omega C v_{oq} + (v_{od}^* - v_{od})(k_{vp} + k_{vi}/s) \\ i_{Lq}^* = i_{oq} + \omega C v_{od} + (v_{oq}^* - v_{oq})(k_{vp} + k_{vi}/s), \end{cases} \quad (17)$$

where i_{Ld}^* and i_{Lq}^* are d axis and q axis component of i_L^* , v_{od} and v_{oq} are d axis and q axis component of v_{abc} , ω is angular frequency of MS, k_{vp} and k_{vi} are proportional and integral coefficient of PI1, s is Laplace operator.

Current inner loop controller makes use of the error between i_L^* and i_L with the similar method as Equation (18) to get v_i^*

$$\begin{cases} v_{id}^* = v_{od} - \omega L i_{Lq} + (i_{Ld}^* - i_{Ld})(k_{ip} + k_{ii}/s) \\ v_{iq}^* = v_{oq} + \omega L i_{Ld} + (i_{Lq}^* - i_{Lq})(k_{ip} + k_{ii}/s), \end{cases} \quad (18)$$

where v_{id}^* and v_{iq}^* are d axis and q axis component of v_i^* , i_{Ld} and i_{Lq} are d axis and q axis component of i_L , k_{ip} and k_{ii} are proportional and integral coefficient of PI2.

Finally, space vector PWM (SVPWM) is used with v_i^* to generate gate signals for inverter to accomplish the control of MS.

5. Simulation analysis

In order to compare the use of two kinds of droop control, MATLAB/Simulink is applied in this part to simulate microgrid islanded operation mode with MS controller design on the basis of the previous part. MS1-3 supply rated power load before 0.6 s, 80% rated power load

during 0.6 s to 0.9 s and again rated power load after 0.9 s. That is to say, load power decreases at 0.6 s and increases at 0.9 s.

Parameters of MS1-3 are shown in Table 1. Their DC bus side voltages are all of 700 V. The length of line1-3 is respectively 0.5 km, 0.4 km and 0.3 km. Line unit length resistance and reactance parameters are $0.642 \Omega/\text{km}$ and $0.083 \Omega/\text{km}$. Cutoff frequency ω_c is 30 rad/s. Load rated real power and reactive power are 20 kW and 10 kvar. In this paper, the ideal power distribution ratio between MS1-3 is 2:1.5:1.

Table 1. Parameters of MS1-3

MS	L / mH	C / μF	S / kVA
MS1	1.5	60	20
MS2	2.0	45	15
MS3	3.0	30	10

In two kinds of droop control, V_{oref} and δ_{ref} are both of 220 V and 0 rad, both droop coefficients are the same and shown in Table 2.

Table 2. Droop coefficients of droop control

m_1	$5.4 \times 10^{-4} \text{ V/W}$
m_2	$7.2 \times 10^{-4} \text{ V/W}$
m_3	$10.8 \times 10^{-4} \text{ V/W}$
n_1	$2.4 \times 10^{-6} \text{ rad/var}$
n_2	$3.2 \times 10^{-6} \text{ rad/var}$
n_3	$4.8 \times 10^{-6} \text{ rad/var}$

Simulation results about output power with traditional droop control are shown in Figure 5.

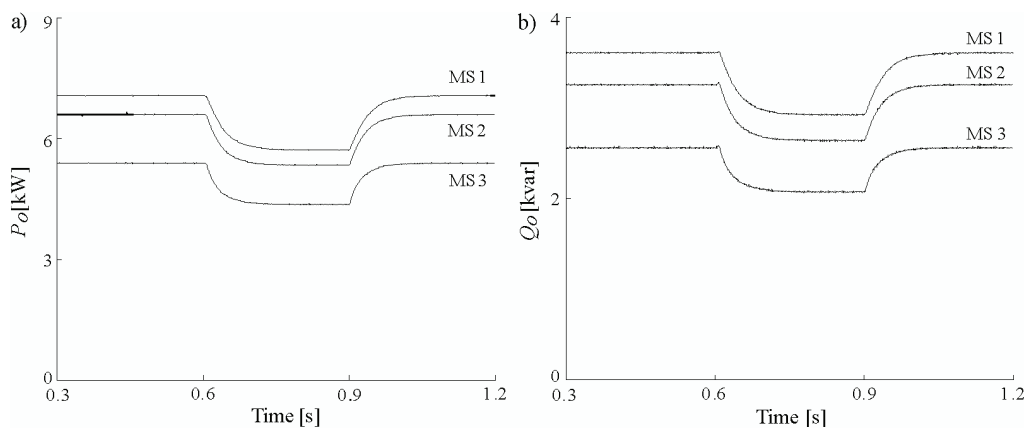


Fig. 5. Output power with traditional droop control: (a) output real power of MS1-3;
(b) output reactive power of MS1-3

When MS1-3 supply rated power load, output real power of MS1-3 is 7.1 kW, 6.6 kW and 5.4 kW. The real power distribution ratio is 1.31:1.22:1. Output reactive power of MS1-3 is 3.6 kvar, 3.3 kvar and 2.6 kvar. The reactive power distribution ratio is 1.38:1.27:1. When MS1-3 supply 80% rated power load, output real power of MS1-3 is 5.7 kW, 5.3 kW and 4.4 kW. The real power distribution ratio is 1.3:1.2:1. Output reactive power of MS1-3 is 2.9 kvar, 2.6 kvar and 2.1 kvar. The reactive power distribution ratio is 1.38:1.24:1. MS1-3 can change their output power to follow load power variation, but the power distribution ratio can not attain desired consequent.

Simulation results about output power with droop control including line compensation are shown in Figure 6. When MS1-3 supply rated power load, output real power of MS1-3 is 8.7 kW, 6.5 kW and 4.3 kW. The real power distribution ratio is 2.02:1.51:1.

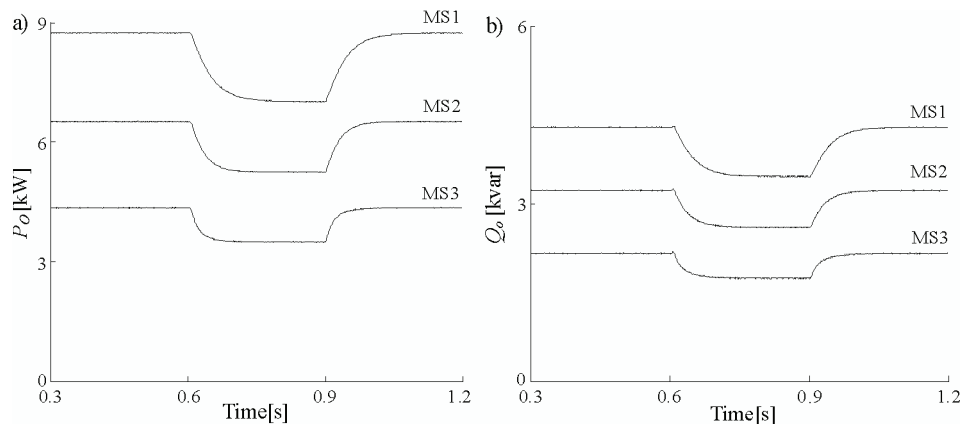


Fig. 6. Output power with droop control including line compensation: (a) output real power of MS1-3; (b) output reactive power of MS1-3

Output reactive power of MS1-3 is 4.3 kvar, 3.2 kvar and 2.2 kvar. The reactive power distribution ratio is 1.95:1.45:1. When MS1-3 supply 80% rated power load, output real power of MS1-3 is 7.0 kW, 5.2 kW and 3.5 kW. The real power distribution ratio is 2.0:1.49:1. Output reactive power of MS1-3 is 3.5 kvar, 2.6 kvar and 1.7 kvar. The reactive power distribution ratio is 2.06:1.53:1. The output power of MS1-3 can not only follow load power variation but also possess relatively expected power distribution ratio.

Simulation results about PCC voltage with droop control including line compensation are shown in Figure 7. Whether load power is constant or not constant, the voltage support of PCC is provided by MS1-3. Figure 7 (a) and (b) indicate that PCC voltage can rapidly stabilize when load power varies. This implies that the voltage control effect of MS controller is desirable. Figure 6 (a) and Figure 7 (c) show that PCC voltage RMS and output real power of MS1-3 have reverse variation. Furthermore, Figure 6 (b) and Figure 7 (d) show that PCC voltage frequency and output reactive power of MS1-3 have same variation. Above phenomenon is reasonable since PCC voltage depends on the output voltage of MS1-3 decided by droop control. When output power of MS1-3 is steady, PCC voltage RMS and frequency are also steady.

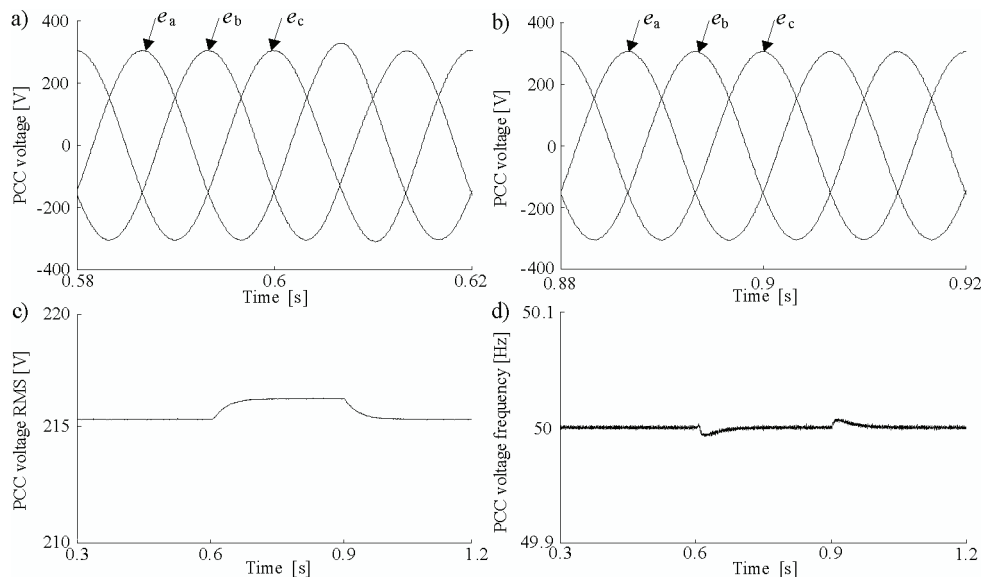


Fig. 7. PCC voltage with droop control including line compensation: (a) PCC voltage waveform when load decreases; (b) PCC voltage waveform when load increases; (c) PCC voltage RMS; (d) PCC voltage frequency

6. Conclusions

This paper focuses on microgrid islanded operation mode with parallel connection of three distributed MSs and one centralized load. The output power of MSs flowing through lines leads to voltage RMS and phase angle difference between MSs and PCC. Traditional droop control is hard to achieve pleased power distribution since it can not overcome this effect. Because droop control including line compensation can remove this effect, MSs using this method can track load power variation with pleased power distribution. MSs provide voltage support for PCC whose voltage RMS is decided by output real power of MSs and frequency by output reactive power of MSs. The output voltage control effect of MSs with the voltage and current dual loop controller is satisfactory.

Acknowledgement

This work was supported by the National High Technology Research and Development Program of China (863 Program) under Grant No. 2011AA050403.

References

- [1] Lasseter R.H., *Microgrids*. Proceedings of IEEE Power Engineering Society Winter Meeting, USA, New York, pp. 305-308 (2002).
- [2] Lasseter R.H., Paigi P., *Microgrid: A Conceptual Solution*. Annual IEEE Power Electronics Specialists Conference, Germany, Aachen, pp. 4285-4290 (2004).

- [3] Pecas Lopes J.A., Moreira C.L., Madureira A.G., *Defining Control Strategies for MicroGrids Islanded Operation*. IEEE Transactions on Power Systems 21(2): 916-924 (2006).
- [4] Katiraei F., Iravani M.R., *Power Management Strategies for a Microgrid With Multiple Distributed Generation Units*. IEEE Transactions on Power Systems 21(4): 1821-1831 (2006).
- [5] Hatziargyriou N., Asano H., Iravani R., Marnay C., *Microgrids: An Overview of Ongoing Research, Development, and Demonstration Projects*. IEEE Power & Energy Magazine 5(4): 78-94 (2007).
- [6] Katiraei F., Iravani R., Hatziargyriou N., Dimeas A., *Microgrids Management: Controls and Operation Aspects of Microgrids*. IEEE Power & Energy Magazine 6(3): 54-65 (2008).
- [7] Li Y., Vilathgamuwa D.M., Loh P.C., *Design, Analysis, and Real-Time Testing of a Controller for Multibus Microgrid System*. IEEE Transactions on Power Electronics 19(5): 1195-1204 (2004).
- [8] Pogaku N., Prodanovic M., Green T.C., *Modeling, Analysis and Testing of Autonomous Operation of an Inverter-Based Microgrid*. IEEE Transactions on Power Electronics 22(2): 613-625 (2007).
- [9] Majumder R., Ghosh A., Ledwich G., Zare F., *Load Sharing and Power Quality Enhanced Operation of a Distributed Microgrid*. IET Renewable Power Generation 3(2): 109-119 (2009).
- [10] Guerrero J.M., Vasquez J.C., Matas J. et al., *Control Strategy for Flexible Microgrid Based on Parallel Line-Interactive UPS Systems*. IEEE Transactions on Industrial Electronics 56(3): 726-736 (2009).
- [11] Tuladhar A., Jin H., Unger T., Mauch K., *Parallel Operation of Single Phase Inverter Modules with no Control Interconnections*. IEEE Applied Power Electronics Conference and Exposition, USA, Atlanta, pp. 94-100 (1997).
- [12] Tuladhar A., Jin H., Unger T., Mauch K., *Control of Parallel Inverters in Distributed AC Power Systems with Consideration of Line Impedance Effect*. IEEE Transactions on Industrial Applications 36(1): 131-138 (2000).
- [13] Li Y., Kao C., *An Accurate Power Control Strategy for Power-Electronics-Interfaced Distributed Generation Units Operating in a Low-Voltage Multibus Microgrid*, IEEE Transactions on Power Electronics 24(12): 2977-2988 (2009).
- [14] Majumder R., Ledwich G., Ghosh A. et al., *Droop Control of Converter-Interfaced Microsources in Rural Distributed Generation*. IEEE Transactions on Power Delivery 25(4): 2768-2778 (2010).
- [15] Engler A., *Applicability of Droops in Low Voltage Grids*. International Journal of Distributed Energy Resources 1(1): 1-5 (2005).
- [16] Engler A., Soultanis N., *Droop Control in LV-Grids*. International Conference on Future Power Systems, Netherlands, Amsterdam 6, pp. 6 (2005).
- [17] Laaksonen H., Saari P., Komulainen R., *Voltage and Frequency Control of Inverter Based Weak LV Network Microgrid*. International Conference on Future Power Systems, Netherlands, Amsterdam 6, pp. 6 (2005).
- [18] Guerrero J.M., Hang L., Uceda J., *Control of Distributed Uninterruptible Power Supply Systems*. IEEE Transactions on Industry Electronics 55(8): 2845-2859 (2008).
- [19] Mohamed Y., El-Saadany E.F., *Adaptive Decentralized Droop Controller to Preserve Power Sharing Stability of Paralleled Inverters in Distributed Generation Microgrids*. IEEE Transactions on Power Electronics 23(6): 2806-2816 (2008).